Published in final edited form as:

Nature. 2015 October 1; 526(7571): 122–125. doi:10.1038/nature15379.

The soft palate is an important site of adaptation for transmissible influenza viruses

Seema S. Lakdawala[1,+], **Akila Jayaraman**[2], **Rebecca A. Halpin**[3], **Elaine W. Lamirande**[1], **Angela R. Shih**[1], **Timothy B. Stockwell**[3], **Xudong Lin**[3], **Ari Simenauer**[3], **Christopher T. Hanson**[1], **Leatrice Vogel**[1], **Myeisha Paskel**[1], **Mahnaz Minai**[4], **Ian Moore**[4], **Marlene Orandle**[4,+], **Suman R. Das**[3], **David E. Wentworth**[3,+], **Ram Sasisekharan**[2,*], and **Kanta Subbarao**[1,*]

[1]Laboratory of infectious Diseases, National Institute of Allergy and Infectious Diseases, National Institutes of Health, Bethesda, Maryland, United States of America

[2]Department of Biological Engineering, Koch Institute for Integrative Cancer Research, Singapore-MIT Alliance for Research and Technology, Massachusetts Institute of Technology, Cambridge, Massachusetts, United States of America

[3]J. Craig Venter Institute, Rockville, Maryland, USA

[4]Comparative Medicine Branch, National Institute of Allergy and Infectious Diseases, National Institutes of Health, Bethesda, Maryland, United States of America

Influenza A viruses (IAV) pose a major public health threat by causing seasonal epidemics and sporadic pandemics. Their epidemiological success relies on airborne transmission (AT) from person-to-person; however, the viral properties governing AT of IAV are complex. IAV infection is mediated via binding of the viral hemagglutinin (HA) to terminally attached α2,3 or α2,6 sialic acids (SA) on cell surface glycoproteins. Human IAV preferentially bind α2,6-linked SA while avian IAV bind α2,3-linked SA on complex glycans on airway epithelial cells[1,2]. Historically, IAV with preferential association with α2,3-linked SA have not transmitted efficiently by the airborne route in ferrets[3,4]. In this study, we observed efficient AT transmission of a 2009 pandemic H1N1 virus (H1N1pdm) engineered to preferentially bind α2,3SA. AT was associated with rapid selection of virus with a change at a single HA site which conferred binding to long-chain α2,6SA, without loss of α2,3SA

[*]All correspondence should be directed to R.S (rams@mit.edu) or K.S (ksubbarao@niaid.nih.gov).
Current Address for SSL: Department of Microbiology and Molecular Genetics University of Pittsburgh School of Medicine, Pittsburgh, PA; for DEW: Virology Surveillance and Diagnosis Branch, Influenza Division, Centers for Disease Control and Prevention, Atlanta GA; for MO: National Institute of Occupational Safety and Health, Centers for Disease Control and Prevention, Morgantown WVA.

Supplementary Information is linked to the online version of the paper at www.nature.com/nature

Author Contributions: S.S.L., A.J., R.S., D. W. and K.S. designed the study. S.S.L., A.J., E.W.L., A.R.S., X. L., A. S., C.T.H, L.V., M.P. and M.M. performed the experiments. S.S.L., R.A.H., T.B.S, I. M., M.O., and S.R.D. analyzed the data. S.S.L. and K.S. wrote the paper.

Accession Codes: The sequences detailed in this manuscript can be found in GenBank under accession numbers CY184674-CY185309.

The authors claim no competing financial interest.

binding. The transmissible virus emerged in experimentally infected ferrets within 24 hours post-infection and was remarkably enriched in the soft palate (SP), where long-chain α2,6SA predominate on the nasopharyngeal surface. Importantly, presence of long-chain α2,6SA is conserved in ferret, pig and human SP. Using a "loss-of-function" approach with this one virus, we demonstrate that the ferret SP, a tissue not normally sampled, rapidly selects for transmissible IAV with human receptor (α2,6SA) preference.

Receptor-binding specificity is an important determinant of host-range restriction and transmission of IAV[4,5] and reviewed in[6]. The ability of zoonotic IAV for AT increases their pandemic potential[7]. Recently, several investigators have attempted to identify viral determinants of AT by generating transmissible H5 and H7 avian IAV[8-10]. We approached the question differently and used an epidemiologically successful IAV in which we altered receptor preference from the human (α2,6SA) to the avian receptor (α2,3SA).

We previously generated H1N1pdm virus variants, with highly specific binding to either α2,6 or α2,3 SA, referred to as α2,6 or α2,3 H1N1pdm respectively[11]. The α2,3 H1N1pdm virus was generated by introducing four amino acid (aa) mutations in the receptor binding site (RBS) of HA (D187E, I216A, D222G, and E224A)[11]. Unexpectedly, the α2,6 and α2,3 H1N1pdm viruses transmitted via AT equally well in ferrets (Fig.1, Supplemental Table1) and with a similar efficiency as observed previously for wild-type H1N1pdm virus[12-15].

A delay in peak viral shedding was noted in the airborne-contact (AC) animals in the α2,3 virus group (red arrows, Fig.1) suggesting that the virus evolves prior to transmission. Deep sequence analysis of viral RNA (vRNA) extracted from nasal washes (NW) of α2,3 H1N1pdm virus-infected ferrets revealed a mixed population at aa 222 (H1 numbering) with the engineered glycine (G) and wild-type aspartic acid (D), while the other three engineered changes in the HA were retained (Fig.2a, Supplemental Table2). Interestingly, the vRNA from the NW of AC ferrets contained only the G222D HA mutation (Fig.2a, Supplemental Table2), suggesting that this sequence at aa 222 in the α2,3 H1N1pdm virus was associated with AT. The virus inoculum did not contain a mixture at this residue (Fig.2a) and associated changes were not observed in the neuraminidase gene (Supplemental Table3).

A D222G change in the 2009 H1N1pdm virus HA has occurred in natural isolates and reports suggest an association with increased virulence in humans and no effect on AT[16-18]. Theoretical structural analysis suggest that the G222D reversion makes the RBS better suited to bind α2,6SA while retaining contacts with α2,3SA via glutamic acid at aa 187 (Extended Data Fig.1). Glycan binding data corroborated this structural prediction because the G222D mutation caused no change in α2,3SA binding but substantially increased binding to long-chain α2,6SA (Fig.2b). Previous reports have demonstrated the importance of α2,6SA binding for transmission[4,5,19]. We now demonstrate conclusively that AT requires gain of long-chain α2,6SA binding and, contrary to previous suggestions[4], loss of α2,3SA binding is not necessary.

The presence of a distinct and identifiable HA sequence in the transmissible virus allowed us to determine whether it emerges in a specific area of the respiratory tract of experimentally infected ferrets. Tissue sections and samples from the upper and lower

respiratory tract were collected on several days post-infection (DPI) from groups of 3 ferrets infected with the α2,3 H1N1pdm virus. Virus was detected in all ferrets and all samples (Extended Data Fig.2). Deep sequencing of vRNA from both the upper and lower respiratory tract revealed a mixed population at residue 222 (Fig.3). Surprisingly, vRNA from the SP was remarkably and uniquely enriched for the G222D virus on 1 DPI and ≥90% of the sequences encoded 222D at 3 DPI (Fig.3c). All other engineered mutations were maintained (Extended Data Fig.3). These data suggest that the G222D revertant virus was actively selected in the ferret SP.

To determine whether the rapid enrichment of G222D revertant virus in the SP was responsible for infection of the AC animal, we performed an AT study where naïve ferrets were exposed to experimentally infected donor ferrets for only 2 days. Surprisingly, even within this shortened exposure time, two AC animals shed virus and 3 out of 4 AC animals seroconverted (Extended Data Fig.4 and Supplemental Table1). Sequence analysis of vRNA from the two AC animals with detectable virus in the NW revealed presence of the G222D revertant. These data suggest that the selection of the α2,3 H1N1pdm virus with the 222D sequence occurs within 3 DPI in the donor ferret and that the AC ferrets were possibly infected with virus originating in the SP because there was nearly complete selection of the G222D mutant by 3 DPI in this tissue.

The SP, with mucosal surfaces facing the oral cavity and nasopharynx, is not usually examined in animal models of influenza. To understand what drives the enrichment of the long-chain α2,6SA-binding α2,3 H1N1pdm virus at this site, we stained the SP with lectins specific for α2,6 or α2,3 SA (Extended Data Fig.5). The ciliated respiratory epithelium (RE) and mucus secreting goblet cells in the RE and submucosal glands (SMG) contained α2,6SA (SNA staining) (Extended Data Fig.5). Expression of α2,3SA (MAL II staining) was present in the connective tissue underlying the RE and in the serous cells of the SMG. Using a purified HA protein (SC18) that selectively binds long-chain α2,6SA[20], we found high expression of long-chain α2,6SA in the SP compared to the trachea and lungs of ferrets (Fig. 4, Extended Data Fig.6). A recent report detailing the glycan profile of the ferret respiratory tract confirms that the SP abundantly expresses α2,6 sialylated LacNAc structures[21], similar to the long-chain α2,6SA recognized by SC18 HA. Interestingly, both the RE and olfactory epithelium (OLF) from the nasal turbinates (NT) of ferrets expressed high levels of long-chain α2,6SA, but the RE of the NT was not enriched for G222D mutant (Fig 3b, Extended Data Fig.6). These data suggest that the SP is unusual in driving selection for the G222D virus.

To determine the relevance for humans, we evaluated the expression of long-chain α2,6SA in the SP of humans and pigs. Interestingly, expression of long-chain α2,6SA was conserved on the RE and goblet cells of the SP of both species (Fig.4). In addition, staining with plant lectins specific for α2,6 or α2,3SA (Extended Data Fig.7) revealed that α2,6SA were present on the nasopharyngeal surface and SMG of both pigs and humans. Expression of α2,3SA was detected in the basal cells of the oral surface and on the nasopharyngeal surface of the human SP; these findings are consistent with reports describing the SA distribution in the human nasopharynx[22]. Other investigators have also reported replication of seasonal and pandemic IAV in tissue sections obtained from the human nasopharynx[23]. Taken together

these data highlight the importance of the nasopharynx, of which the SP forms the floor, as a site for host adaptation of IAV.

IAV infection of the SP may contribute to AT by providing a mucin-rich microenvironment for generation of airborne virus during coughing, sneezing or breathing. Infection with α2,3 H1N1pdm virus resulted in severe inflammation and necrosis of the RE cells and SMG in the SP (Extended Data Fig.8). Since the SP is innervated by the trigeminal nerve, inflammation of this tissue could stimulate sneezing. Alternatively, the SP may be the site where infection is initiated during AT; therefore binding to this tissue would provide a fitness advantage.

These results, albeit with one virus enhance our understanding of the properties necessary for AT of IAV in the ferret model. Loss of α2,3SA specificity is not necessary but gain of long-chain α2,6SA binding is critical for efficient AT of IAV. H7N9 viruses from China show dual receptor binding but variable AT efficiency in ferrets[24,25]. Interestingly, the 1918 H1N1 virus (A/New York/1/18), which has a similar SA binding preference as the α2,3 H1N1pdm virus, did not transmit via the airborne route or adapt within the ferret host[4], suggesting that H1N1pdm virus may be unusual for this rapid adaptation. However, Pappas et al recently reported the detection of a mutation that enhanced α2,6SA binding in nasal washes of ferrets infected with avian H2 viruses[26], demonstrating that rapid adaptation of IAV to gain human receptor preference occurs in other IAV subtypes as well.

Studies with transmissible H5 viruses suggest that increased pH and thermal stability of the HA enhance AT[8,9,27]. Although we did not observe adaptive mutations in the HA stalk of the α2,3 H1N1pdm virus, perhaps because H1N1pdm HA is already adapted to humans, a mixed population was observed at four lysine residues around the RBS (Extended Data Fig. 9, Supplemental Table2). Some are known to be egg adaptive mutations[28] or are components of the proposed positively charged ‘lysine fence’ around the base of the RBS, positioned to anchor the N-acetylneuraminic acid and galactose sugar of α2,3 and α2,6SA glycans[29]. Interestingly, the lysine residues were restored in the vRNA isolated from NW of AC ferrets and the SP of experimentally infected ferrets (Extended Data Fig.9,10).

Taken together with our previously published data, long-chain α2,6SA binding and a highly active neuraminidase contribute to the AT of the H1N1pdm virus[12,30]. Importantly, we have identified the previously overlooked SP as an important site of isolation of transmissible virus and perhaps the initial site of infection. Analysis of the replicative fitness of IAV in this tissue may be warranted in assessment of their pandemic potential.

Materials and Methods

Ethics Statement and Animal Studies

This study was carried out in strict accordance with the recommendations in the Guide for the Care and Use of Laboratory Animals of the National Institutes of Health. The National Institutes of Health Animal Care and Use Committee (ACUC) approved the animal experiments that were conducted. All studies were conducted under ABSL2 conditions and all efforts were made to minimize suffering. In our animal study protocol, we state that the

number of animals in each experimental group varies, and is based on our prior experience. We use the minimum number of animals per group that will provide meaningful results. Randomization was not used to allocate animals to experimental groups and the animal studies were not blinded.

Virus Rescue

The 2009 H1N1pdm virus used in this study is A/California/07/2009. Generation and characterization of the α2,3 H1N1pdm and α2,6 H1N1pdm viruses has been described previously[11]. Genomic sequencing and dose dependent glycan binding assays confirmed the identity and receptor specificity of viruses generated by reverse genetics. All experiments were performed using viruses passaged no more than 3 times in MDCK cells or eggs.

Ferret Transmission Study

All ferrets (Mustela putorius furo) were screened by hemagglutination inhibition (HAI) assay prior to infection to ensure that they were naïve to seasonal influenza A and B viruses and the viruses used in this study. The transmission studies were conducted in adult ferrets as previously described[12], male and female ferrets were used in a 3:1 ratio and sample size was based on the capacity of the transmission cages. Ferrets reaching 15-20% weight loss were provided with enriched diet and monitored closely by veterinarian staff for altered behavior.

Environmental conditions inside the laboratory were monitored daily and were consistently 19±1°C and 56±2% relative humidity. The transmission experiments were conducted in the same room, to minimize any effects of caging and airflow differences on aerobiology. On day 0 four animals were infected intranasally with 10^6 $TCID_{50}$ of either α2,3 H1N1pdm or α2,6 H1N1pdm virus and placed into the transmission cage. Twenty-four hours post-infection, a naïve animal (airborne-contact or AC) was placed into the transmission cage on the other side of a perforated stainless steel barrier. The AC ferrets were always handled before the infected ferrets. Nasal washes were collected and clinical signs were recorded on alternate days from days 0 to 14. Great care was taken during nasal wash collections and husbandry to ensure that direct contact did not occur between the ferrets. On 14 days post-infection (DPI), blood was collected from each animal for serology. The shortened exposure time study was done similarly except 48 hours after the naïve recipient animal (Airborne contact - AC) was placed into the transmission cage the ferrets were separated into micro-isolator cages. Infected ferrets were sacrificed on 7 DPI and the AC animals were sacrificed on 21 DPI. The AC animals were always handled before infected ferrets and all husbandry tools were decontaminated three times between handling of each AC animal.

Dose dependent direct binding of influenza viruses

To determine the receptor specificity of the G222D α2,3 H1N1pdm virus, virus from the nasal wash of a single AC animal on day 6 post-exposure was propagated once in MDCK cells. This virus stock was inactivated with betapropiolactone (BPL) and the hemagglutination titer was determined. For the glycan binding assay, 50μl of 2.4 μM biotinylated glycans were added to wells of streptavidin-coated high binding capacity 384-well plates (Pierce) and incubated overnight at 4°C. The glycans included were 3′SLN,

3′SLN-LN, 3′SLN-LN-LN, 6′SLN and 6′SLN-LN (LN corresponds to lactosamine (Galβ1-4GlcNAc) and 3′SLN and 6′SLN respectively correspond to Neu5Acα2-3 and Neu5Acα2-6 linked to LN) that were obtained from the Consortium of Functional Glycomics (www.functionalglycomics.org). The inactivated G222D virus was diluted to 250 μl with 1X PBS + 1% BSA. 50 μl of diluted virus was added to each of the glycan-coated wells and incubated overnight at 4 °C. This was followed by three washes with 1X PBST (1X PBS + 0.1% Tween-20) and three washes with 1X PBS. The wells were blocked with 1X PBS + 1% BSA for 2 h at 4 °C followed by incubation with primary antibody (ferret anti – CA07/09 antisera; 1:200 diluted in 1X PBS + 1% BSA) for 5 h at 4 °C. This was followed by three washes with 1X PBST and three washes with 1X PBS. Finally, the wells were incubated with the secondary antibody (goat anti-ferret HRP conjugated antibody from Rockland; 1:200 diluted in 1X PBS + 1% BSA). The wells were washed with 1X PBST and 1X PBS as before. The binding signals were determined based on the HRP activity using the Amplex Red Peroxidase Assay (Invitrogen) according to the manufacturer's instructions. Negative controls were uncoated wells (without any glycans) to which just the virus, the antisera and the antibody were added and glycan coated wells to which only the antisera and the antibody were added.

Ferret Replication

We evaluated the replication kinetics of the α2,3 H1N1pdm virus in the respiratory tract of 6-8 month old male ferrets as previously described[11]. Briefly, all ferrets were screened prior to infection by HAI assay to ensure that they were naïve to seasonal influenza A and B viruses. Animals were infected intranasally with 10^6 $TCID_{50}$ of α2,3 H1N1pdm virus in 500μl. Tissues were harvested to assess viral titers. Tissues were weighed and homogenized in Leibovitz's L-15 (L-15, Invitrogen) at 5% (nasal turbinates and trachea) or 10% (lung) weight per volume (W/V). The soft palate was homogenized in 1 mL of L-15. Clarified supernatant was aliquoted and titered on MDCK cells. The 50% tissue culture infectious dose ($TCID_{50}$) per gram of tissue was calculated by the Reed and Muench method [31].

Influenza A virus Full genome Sequencing

The influenza A genomic RNA segments were simultaneously amplified from 3 μl of purified RNA (from homogenized ferret tissue) using a multi-segment RT-PCR strategy (M-RTPCR) [32]. In a separate reaction, each HA segment was amplified using HA-specific primers (swH1ps-1A-F: 5′-AGCAAAAGCAGGGGAAAACAAAAGCAAC-3′;swH1ps-1777A-R: 5′-AGTAGAAACAAGGGTGTTTTTCTCATGC-3′). Analysis of influenza viral RNA from ferret trachea and region of nasal turbinates enriched for respiratory epithelium (RE), between the canine and 2nd premolar teeth, was collected from tissue stored in RNAlater (Ambion) and total RNA was extracted using RNAeasy Kit (Qiagen). For these samples, nested HA-specific small amplicons were generated using HA-specific PCR primers (Outer primer pair H1-399F: 5′-AGCTCAGTGTCATCATTTGAAAG-3′ and H1-961R: 5′-TGAAATGGGAGGCTGGTGTT-3′; and inner primer pair H1-468 F:5′-AACAAAGGTGTAACGGCAGC-3′ and H1-884R: 5′-AATGATAATACCAGATCCAGCAT-3′). Illumina libraries were prepared from M-

RTPCR products and from HA-specific RT-PCR products using the Nextera DNA Sample Preparation Kit (Illumina, Inc., San Diego, CA, USA) with half-reaction volumes.

After PCR amplification, 10 μl of each library derived from M-RTPCR products was pooled into a 1.5 mL tube; separately, 10 μl of each library derived from HA-specific amplicons was pooled into a 1.5 mL tube. Each pool was cleaned two times with Ampure XP Reagent (Beckman Coulter, Inc., Brea, CA, USA) to remove all leftover primers and small DNA fragments. The first and second cleanings used 1.2× and 0.6× volumes of Ampure XP Reagent, respectively. The cleaned pool derived from M-RTPCR products was sequenced on the Illumina HiSeq 2000 instrument (Illumina, Inc.) with 100-bp paired-end reads, while the cleaned pool derived from HA-specific amplicons was sequenced on the Illumina MiSeq v2 instrument with 300-bp paired-end reads. For additional sequencing coverage, and the HA specific small amplicons, samples were re-sequenced using the Ion Torrent platform. M-RTPCR products were sheared for 7 min, and Ion-Torrent-compatible barcoded adapters were ligated to the sheared DNA using the Ion Xpress Plus Fragment Library Kit (Thermo Fisher Scientific, Waltham, MA, USA) to create 400-bp libraries. Libraries were pooled in equal volumes and cleaned with the Ampure XP Reagent. Quantitative PCR was performed on the pooled, barcoded libraries to assess the quality of the pool and to determine the template dilution factor for emulsion PCR. The pool was diluted appropriately and amplified on Ion Sphere Particles (ISPs) during emulsion PCR on the Ion One Touch 2 instrument (Thermo Fisher Scientific). The emulsion was broken, and the pool was cleaned and enriched for template-positive ISPs on the Ion One Touch ES instrument (Thermo Fisher Scientific). Sequencing was performed on the Ion Torrent PGM using a 318v2 chip (Thermo Fisher Scientific).

Deep sequencing analysis

Deep sequencing preparation, collection, and analysis was conducted by investigators who were blinded to the experimental groups. For virus sequence assembly, all sequence reads were sorted by barcode, trimmed, and *de novo* assembled using CLC Bio's *clc_novo_assemble* program (Qiagen, Hilden, Germany). The resulting contigs were searched against custom full-length influenza segment nucleotide databases to find the closest reference sequence for each segment. All sequence reads were then mapped to the selected reference influenza A virus segments using CLC Bio's *clc_ref_assemble_long* program.

Minor allele variants were identified using *FindStatisticallySignificantVariants* (*FSSV*) software (http://sourceforge.net/projects/elvira/). The *FSSV* software applies statistical tests to minimize false-positive SNP calls generated by Illumina sequence-specific errors (SSEs) described in[33]. SSEs usually result in false SNP calls if sequences are read in one sequencing direction. The *FSSV* analysis tool requires observing the same SNP at a statistically significant level in both sequencing directions. Once a minimum minor allele frequency threshold and significance level are established, the number of minor allele observations and major allele observations in each direction and the minimum minor allele frequency threshold are used to calculate p-values based on the binomial distribution cumulative probability. If the p-values calculated in both sequencing directions are less than

the Bonferroni-corrected significance level, then the SNP calls are accepted. A significance level of 0.05 (Bonferroni-corrected for tests in each direction to 0.025) and a minimum minor allele frequency threshold of 3% were applied for this analysis. Differences in the consensus sequence compared to the reference sequence were identified using CLC Bio's *find_variations* software. The identified consensus and minor allele variations were analyzed by assessing the functional impact on coding sequences or other regions based on overlap with identified features of the genome. For each sample, the reference sequence was annotated using *VIGOR* software[34], and then the variant data and genome annotation were combined using *VariantClassifier* software[35] to produce records describing the impacts of the identified variations.

Lectin and Immuno Histochemistry

Lectin histochemistry was performed as described previously for plant lectins[36] and purified HA protein[37]. For plant lectin staining, the soft palate was subjected to microwave-based antigen retrieval using a citrate buffer and was then incubated with FITC-conjugated *Sambucus nigra* agglutinin (SNA) and biotinylated *Maackia amurensis* agglutinins (MAL II) lectins (Vector Laboratories), followed by a streptavidin-Alexa-Fluor594 conjugate (Invitrogen). For SC18 staining, the tissue sections were incubated with precomplexed purified His-tagged SC18 HA protein, mouse anti-His antibody (Abcam), and goat anti-mouse IgG secondary antibody conjugated to Alexa-Fluor 488 (Molecular Probes) at a 4:2:1 ratio. Nuclei were counter stained with DAPI (Vector Laboratories) and sections were mounted with either ProLong Gold anti-fade reagent (Invitrogen) or Fluoromount-G (Southern Biotech). Images were captured either on an Olympus BX51 microscope with an Olympus DP80 camera or a Leica SP5 confocal microscope.

Ferret nasal turbinate biopsy samples were obtained from an uninfected ferret 8 months old as follows: the head was dissected sagittally to expose two halves of the ferret nasal turbinates, biopsy of turbinates between the canine and 2nd premolar represented respiratory epithelium (RE) and biopsy of turbinates at the molar tooth represented olfactory epithelium (OLF). A schematic depicting these two areas is shown in extended data figure 5H. Pig soft palate tissue sections were a kind gift from Dr. XJ Meng (Virginia Tech College of Veterinary Medicine) and Dr. Pablo Pineyro (Iowa State University). Pig soft palate tissues were collected from four 56 day-old mixed-breed commercial swine and fixed in 10% formalin. Soft palate tissues from four adult cadavers were obtained from the Maryland State Anatomy Board, Department of Heath and Mental Hygiene in Baltimore, MD.

Extended Data

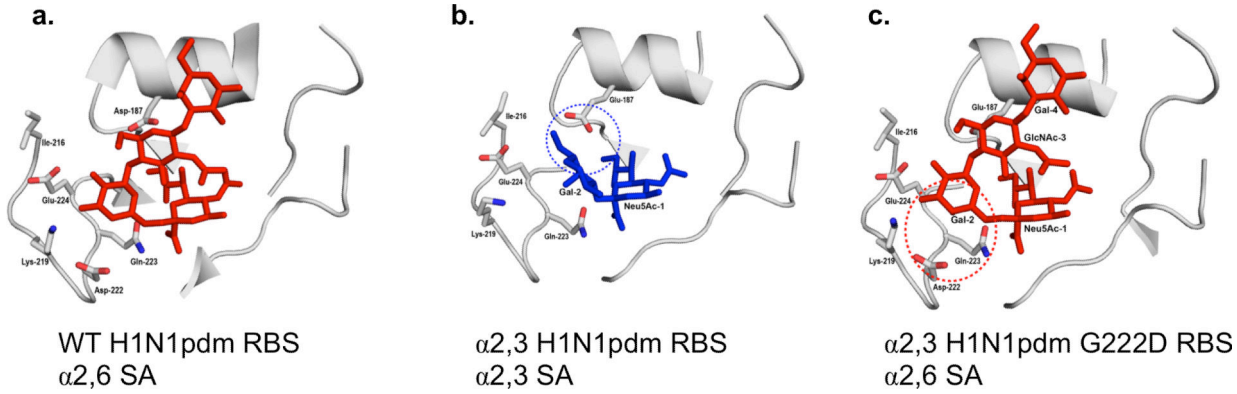

Extended Data Fig. 1. Amino acids in the receptor binding site of H1N1pdm HA that bind to α2,3 and α2,6 glycans

Ribbon diagrams of the 2009 H1N1pdm HA receptor binding pocket interacting with an α2,6 sialic acid in the pocket (**a**), an α2,3 H1N1pdm HA with α2,3 glycan (**b**), or α2,3 G222D revertant H1N1pdm HA and α2,6 sialic acid (**c**).

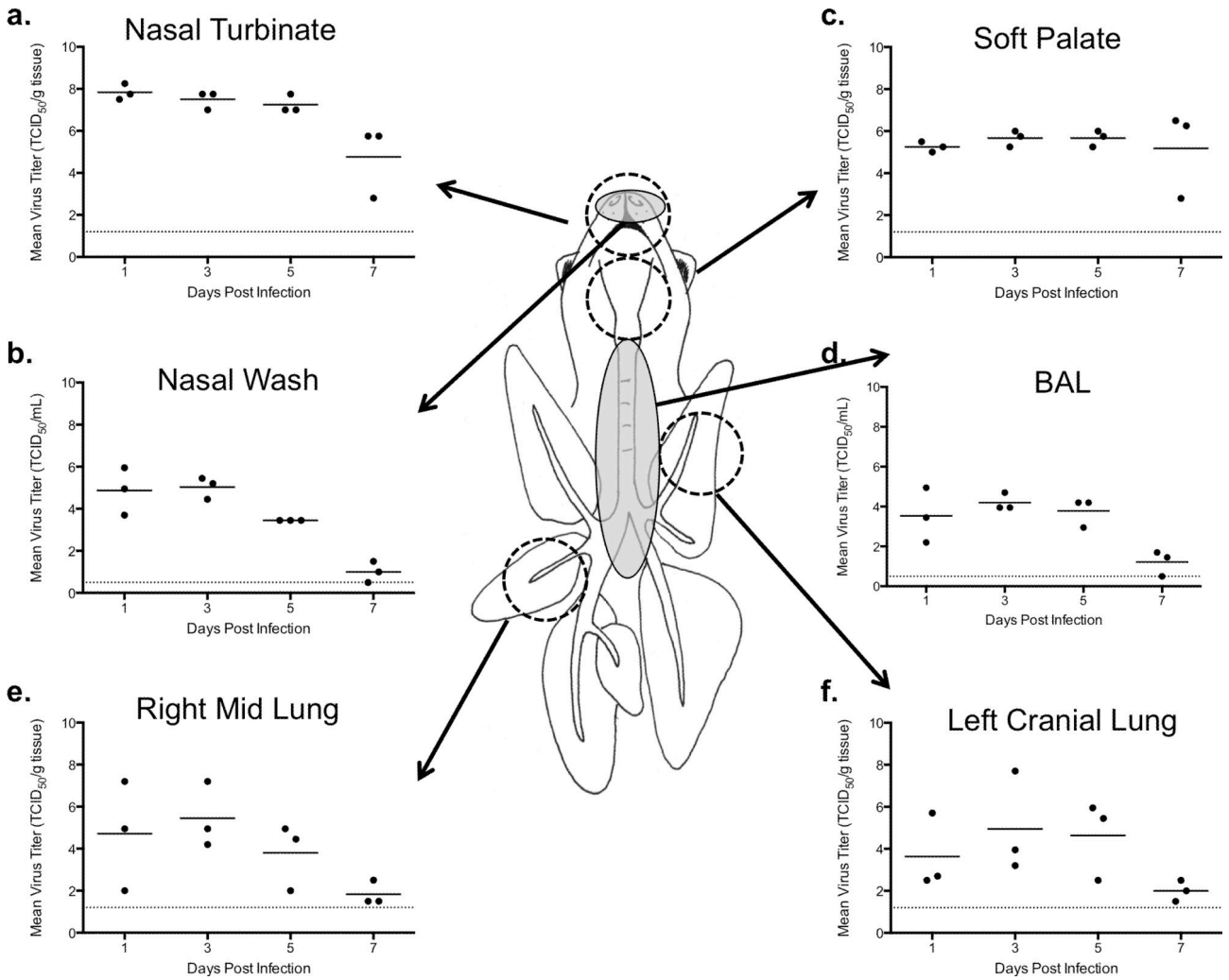

Extended Data Fig. 2. Replication of α2,3 H1N1pdm virus in ferret respiratory tract

We confirmed that the α2,3 H1N1pdm virus replicated to high titers on days 1, 3, and 5 in different parts of the ferret respiratory tract. Each tissue homogenate is highlighted with a dashed-circle, the gray circles represent washes. Each point represents a single animal. The horizontal black line indicates the mean viral titer on a given day.

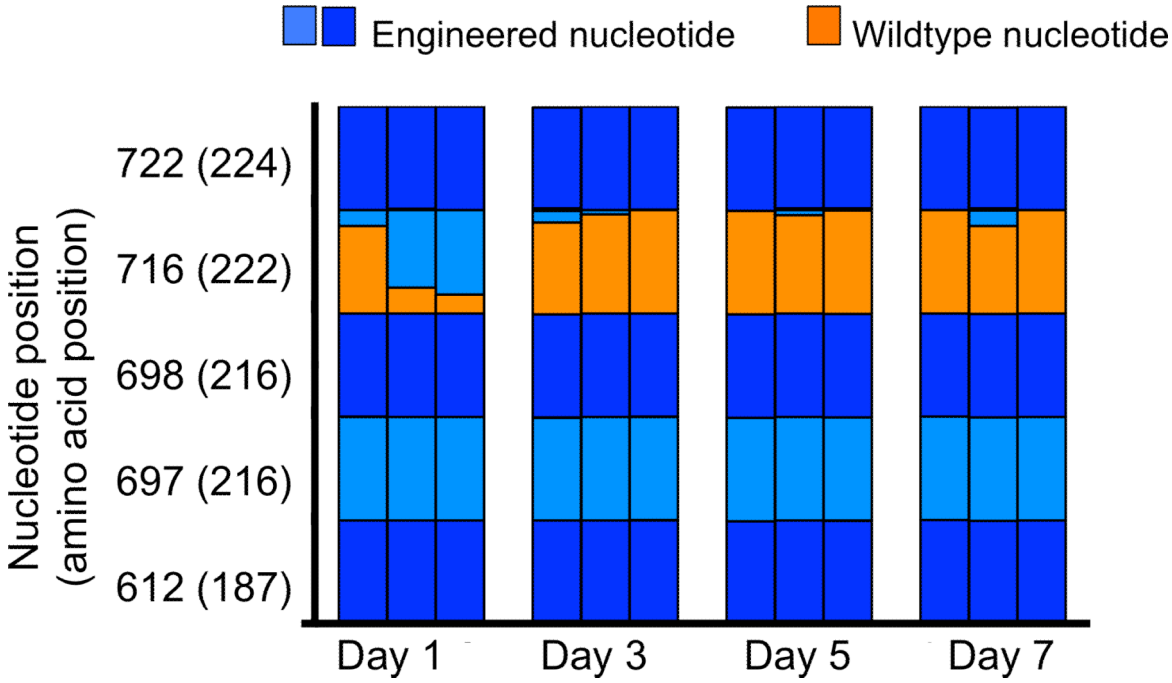

Extended Data Fig. 3. Stability of engineered mutations in viruses replicating in the soft palate

Deep sequencing of the HA gene segment from virus populations in the soft palate from 1, 3, 5, and 7 DPI reveals a rapid change at position 222, but no change in the other engineered sites. The engineered sites are highlighted in blue, while the wild-type nucleotide is in orange. Each bar represents a single animal.

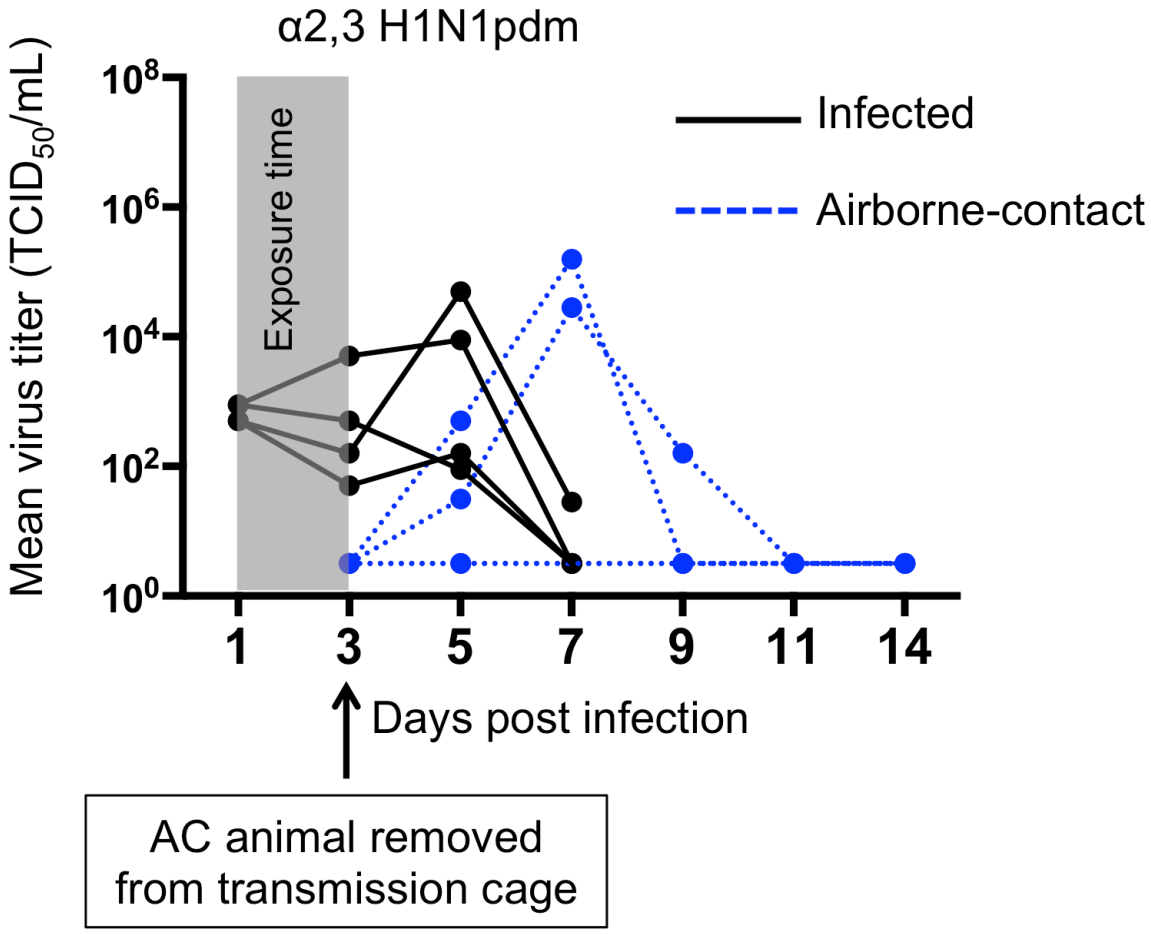

Extended Data Fig. 4. Airborne transmission of α2,3 H1N1pdm virus after 48 hour exposure time

One ferret in each pair was infected with 10^6 $TCID_{50}$ of the indicated virus, a naïve ferret (referred to as airborne-contact or AC) was introduced into the adjacent compartment 24 hours later. The AC animal was removed from the transmission cage on day 3 post-infection as indicated by the black arrow. Nasal secretions were collected every other day for 14 days. Viral titers from the nasal secretions are graphed for each infected or AC animal. The gray shading indicates the exposure time between the infected and AC animals.

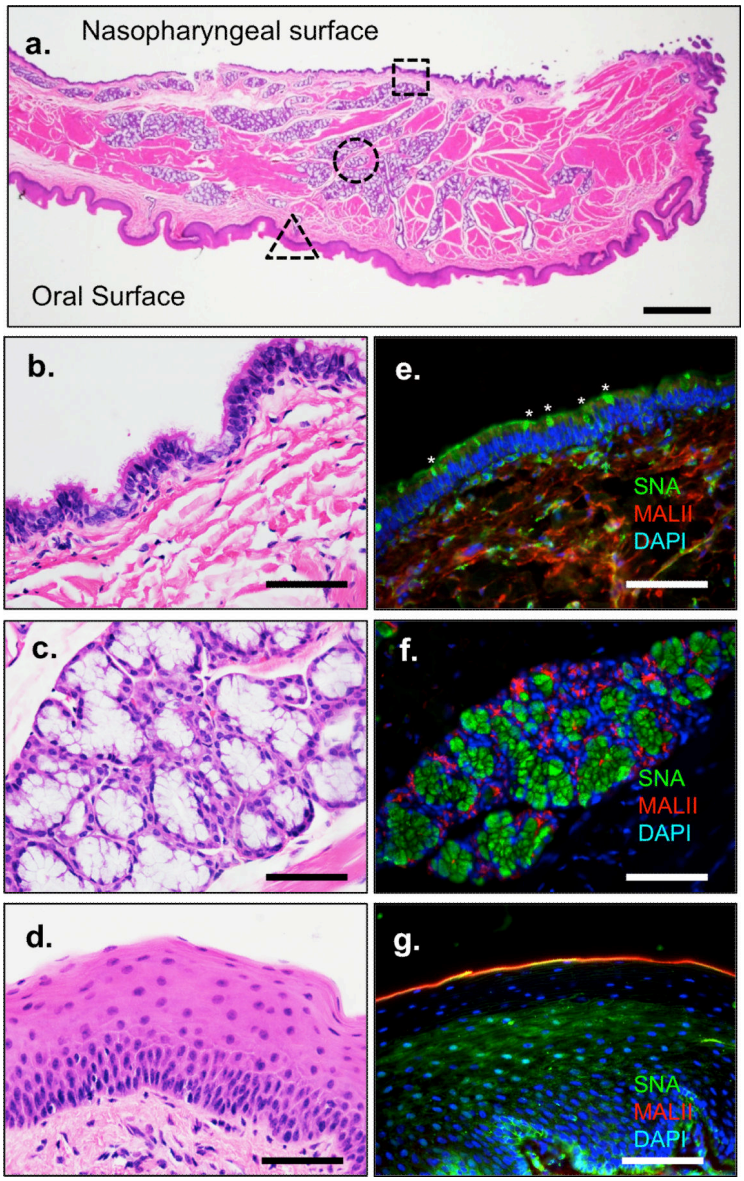

Extended Data Fig. 5. Influenza receptor distribution on ferret soft palate

Hematoxylin and eosin (H&E) staining of the soft palate from an uninfected ferret highlights the nasopharyngeal and oral surfaces. Scale bar is 1.25mm. (**a**) Areas highlighted in parts **b-g** are marked with dashed line shapes: square – nasopharyngeal surface (**b** and **e**), circle - submucosal gland (**d** and **g**) and triangle - oral surface (**c** and **f**). H&E staining of these regions, reproduced from Figure 4A-C in the main text, are shown in b-d. Staining with plant lectins specific for α2,6 SA (SNA) and α2,3 SA (MAL II) are shown in **e-g**. Scale bars are 100μm in images **b-g**.

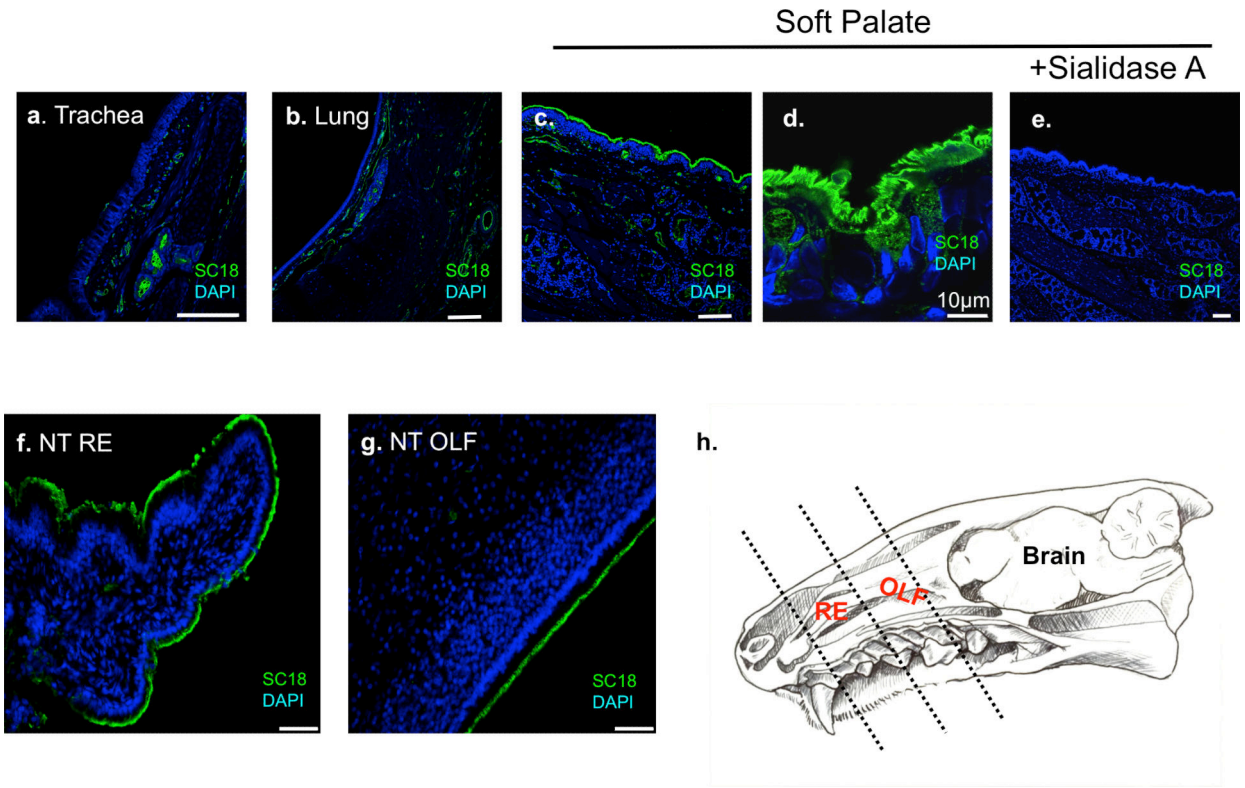

Extended Data Fig. 6. SC18 staining of ferret respiratory tissues

Sections of ferret trachea (**a**) lung (**b**), soft palate (**c** and **d**), biopsy of nasal turbinate tissue with respiratory epithelium (RE) (**f**) and olfactory epithelium (OLF) (**g**) were stained with purified SC18 HA protein to identify areas expressing long-chain α2,6 SA. Illustration of ferret head (sectioned along the midline) highlighting the anatomical locations of RE and OLF tissues is depicted in (**h**). Goblet cells on the respiratory epithelium of the soft palate (nasopharyngeal surface) also stained positive for SC18 (**d**). Absence of SC18 staining after sialidase A treatment (**e**) indicates the high specificity of SC18 for the respiratory epithelium of the soft palate. All scale bars are 100μm unless indicated.

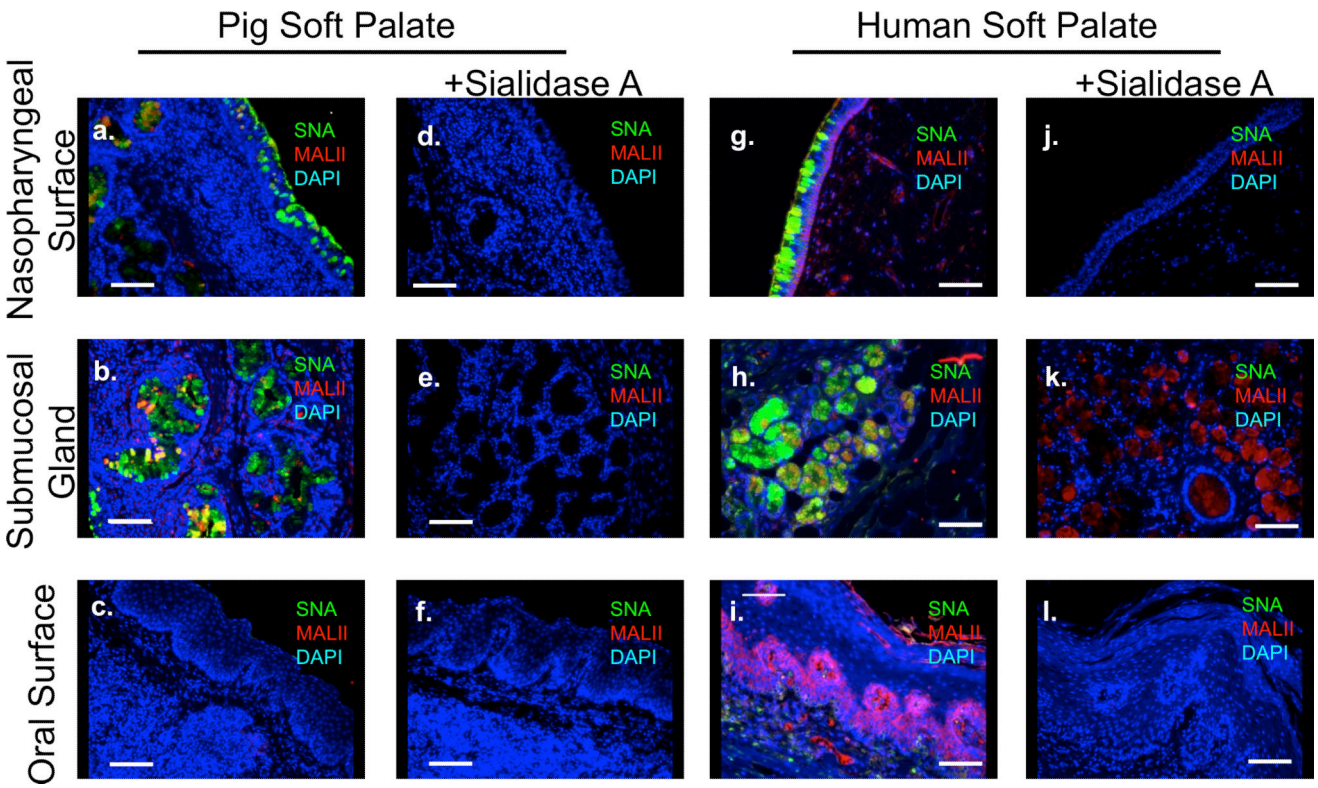

Extended Data Fig. 7. Influenza receptor distribution on pig and human soft palate

Pig (**a-c**) and human (**g-i**) soft palate tissues were stained with plant lectins SNA and MALII which are commonly used as markers for α2,6 and α2,3 sialic acid respectively. Sialidase A treated control was run for each sample to ensure specificity of plant lectins and are displayed in panels (**d-f** and **j-l**). Expression of α2,6 sialic acids (SNA staining) is found on the ciliated respiratory epithelium and goblet cells of the nasopharyngeal surface and in the submucoasl glands of both the pig and human soft palate. Expression of α2,3 sialic acids is low in the pig soft palate and found primarily in goblet cells and submucosal glands. In the human soft palate, MALII (α2,3 sialic acids) staining sensitive to sialidase A treatment is found in the goblet cells and respiratory epithelium of the nasopharyngeal surface and in the basal cells of the oral surface. MALII staining in the submucosal glands was not sensitive to sialidase A treatment. Scale bars are 100μm in all images.

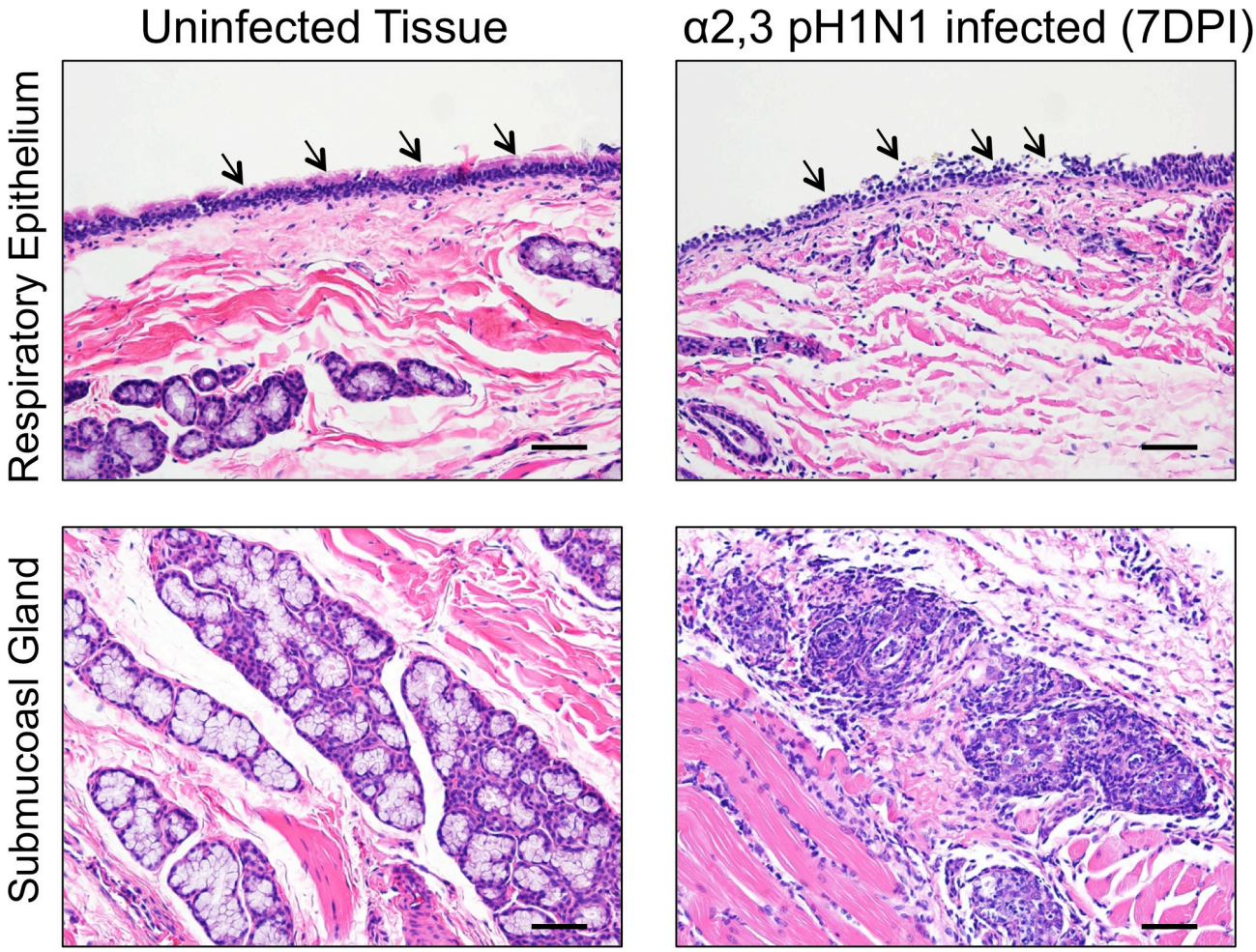

Extended Data Fig. 8. Pathology of the soft palate during infection with α2,3 H1N1pdm

The soft palate was removed from 3 ferrets infected with α2,3 pH1N1 virus on 7 DPI. The tissue sections were stained with hematoxylin and eosin. Black arrows indicate the ciliated respiratory epithelium of the soft palate tissue (nasopharyngeal surface). Scale bars are 100μm in all images.

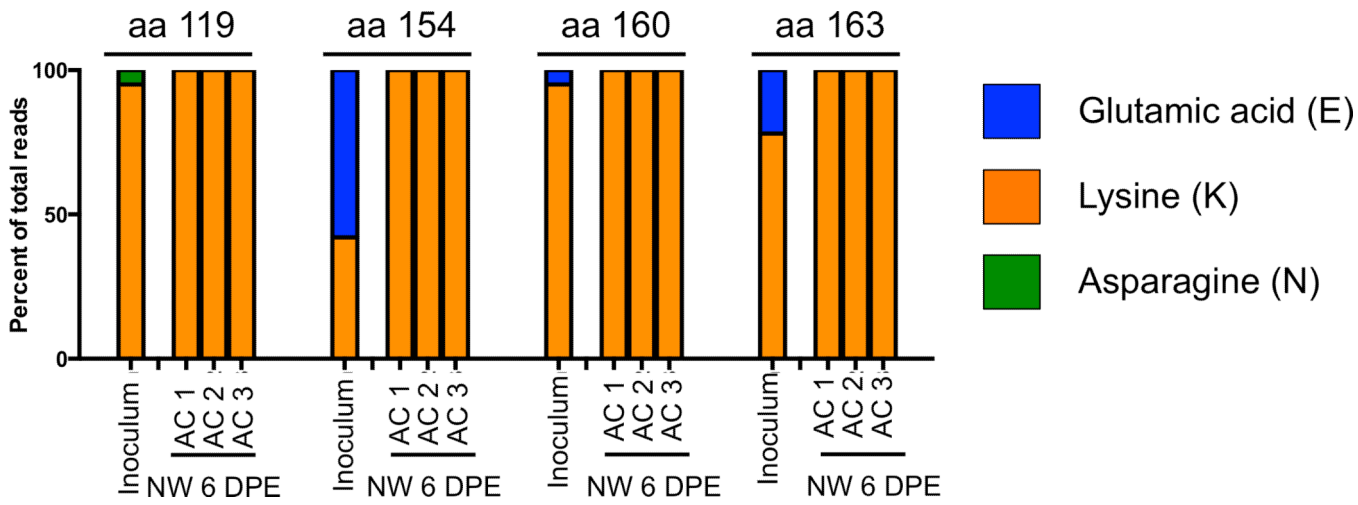

Extended Data Fig. 9. Quasispecies in putative lysine fence

Deep sequencing analysis of the α2,3 H1N1pdm inoculum revealed a mixed population at 4 lysine residues surrounding the receptor binding site of the HA protein. The lysine fence was restored in viruses from the nasal wash of AC animals from 6 days post-exposure (DPE). Each bar represents a single animal, and each amino acid (aa) that contained a quasispecies is indicated.

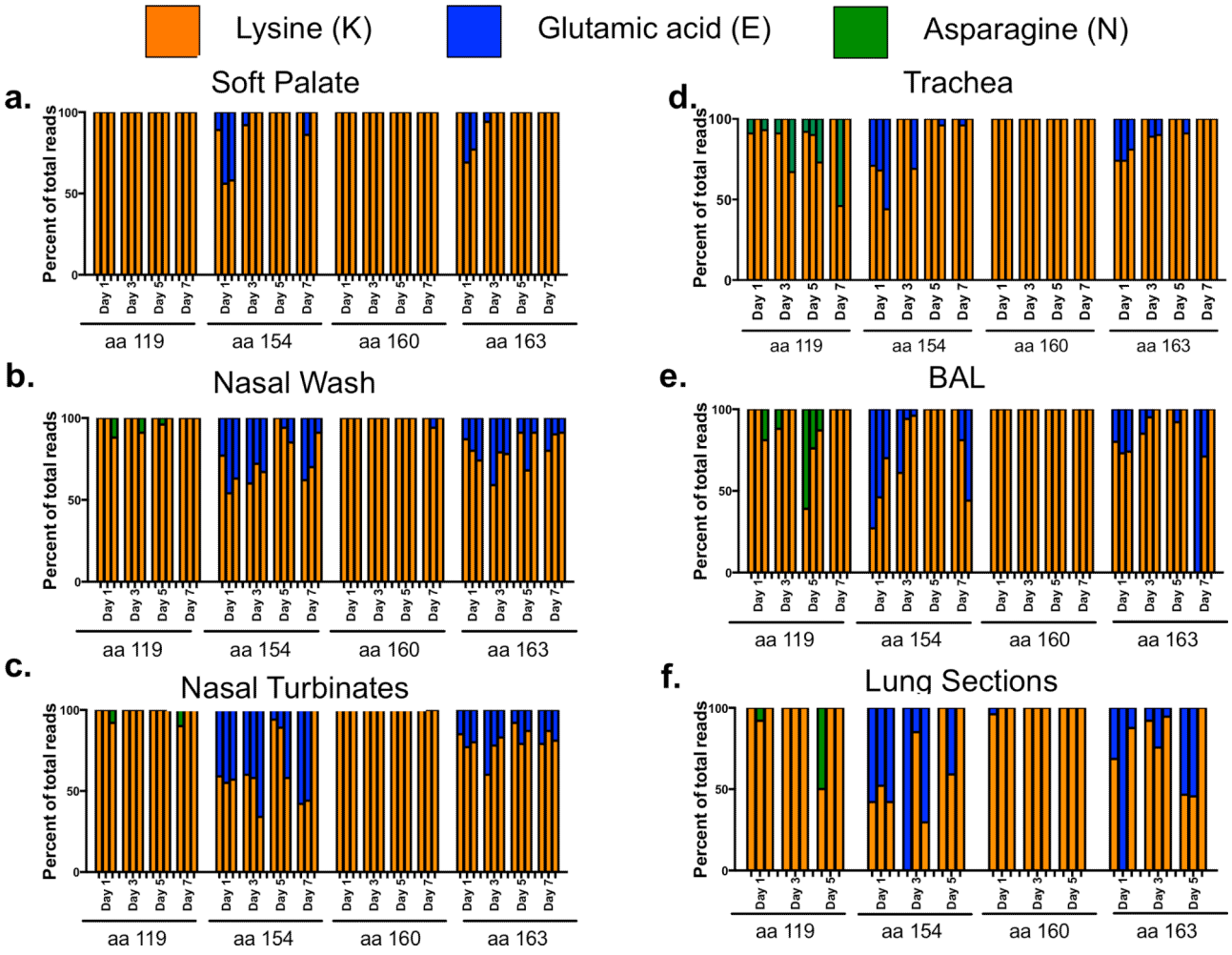

Extended Data Fig. 10. Quasispecies of lysine fence in various ferret respiratory tissue sections

Deep sequencing of viruses from respiratory tissues of ferrets infected with α2,3 H1N1pdm. Viruses populations from the soft palate (**a**), nasal wash (**b**), nasal turbinates (**c**), trachea (**d**), bronchoalveolar lavage (BAL) (**e**), or lung sections (**f**) were analyzed and the proportion of lysine, glutamic acid, or asparagine are presented. Each bar represents a single animal. The lung section is an average of the right middle lung lobe and a portion of the left caudal lung tissue.

Supplementary Material

Refer to Web version on PubMed Central for supplementary material.

Acknowledgments

This research was supported in part by the Intramural Research Program of NIAID, NIH and with federal funds from NIAID, NIH, DHHS under contract number HHSN272200900007C and NIAID/NIH Genomic Centers for Infectious Diseases (GCID) program (U19-AI-110819). This manuscript was reviewed by the NIH's Intramural Research Program's Committee on Dual Use Research of Concern (DURC), who concluded that the methods and results do not meet DURC criteria. We thank the NIAID Comparative Medical Branch for technical assistance, Subbarao lab members for critical input, Nadia B. Fedorova from JCVI for technical help, Dr. XJ Meng (Virginia Tech College of Veterinary Medicine) and Dr. Pablo Pineyro (Iowa State University) for pig soft palate tissues, and

the Consortium for Functional Glycomics for providing glycans for the glycan array analysis. The data for this manuscript and its preparation was generated while DEW was employed at JCVI. The opinions expressed in this article are the authors' own and do not reflect the views of the Centers for Disease Control, the Department of Health and Human Services, or the United States government. AJ and RS are supported in part by NIH Merit Award (R37 GM057073-13), National Research Foundation supported Interdisciplinary Research group in Infectious Diseases of SMART (Singapore MIT alliance for Research and Technology) and the Skolkovo Foundation supported Infectious Diseases Center at MIT.

References

1. Shinya K, et al. Avian flu: influenza virus receptors in the human airway. Nature. 2006; 440:435–436. [PubMed: 16554799]
2. van Riel D, et al. H5N1 Virus Attachment to Lower Respiratory Tract. Science. 2006; 312:399. [PubMed: 16556800]
3. Maines TR, et al. Lack of transmission of H5N1 avian-human reassortant influenza viruses in a ferret model. Proc Natl Acad Sci U S A. 2006; 103:12121–12126. [PubMed: 16880383]
4. Tumpey TM, et al. A two-amino acid change in the hemagglutinin of the 1918 influenza virus abolishes transmission. Science. 2007; 315:655–659. [PubMed: 17272724]
5. Pappas C, et al. Receptor specificity and transmission of H2N2 subtype viruses isolated from the pandemic of 1957. PloS One. 2010; 5
6. Cauldwell AV, Long JS, Moncorge O, Barclay WS. Viral determinants of influenza A virus host range. Journal of General Virology. 2014; 95:1193–1210. [PubMed: 24584475]
7. Lakdawala SS, Subbarao K. The Ongoing Battle Against Influenza: The challenge of flu transmission. Nature Medicine. 2012; 18:1468–1470.
8. Herfst S, et al. Airborne transmission of influenza A/H5N1 virus between ferrets. Science. 2012; 336:1534–1541. [PubMed: 22723413]
9. Imai M, et al. Experimental adaptation of an influenza H5 HA confers respiratory droplet transmission to a reassortant H5 HA/H1N1 virus in ferrets. Nature. 2012; 486:420–428. [PubMed: 22722205]
10. Sutton TC, et al. Airborne Transmission of Highly Pathogenic H7N1 Influenza Virus in Ferrets. Journal of Virology. 2014; 88:6623–6635. [PubMed: 24696487]
11. Lakdawala SS, et al. Receptor specificity does not affect replication or virulence of the 2009 pandemic H1N1 influenza virus in mice and ferrets. Virology. 2013; 446:349–356. [PubMed: 24074599]
12. Lakdawala SS, et al. Eurasian-origin gene segments contribute to the transmissibility, aerosol release, and morphology of the 2009 pandemic H1N1 influenza virus. PLoS Pathogens. 2011; 7
13. Itoh Y, et al. In vitro and in vivo characterization of new swine-origin H1N1 influenza viruses. Nature. 2009; 460:1021–1025. [PubMed: 19672242]
14. Maines TR, et al. Transmission and pathogenesis of swine-origin 2009 A(H1N1) influenza viruses in ferrets and mice. Science. 2009; 325:484–487. [PubMed: 19574347]
15. Munster VJ, et al. Pathogenesis and transmission of swine-origin 2009 A(H1N1) influenza virus in ferrets. Science. 2009; 325:481–483. [PubMed: 19574348]
16. Liu Y, et al. Altered receptor specificity and cell tropism of D222G hemagglutinin mutants isolated from fatal cases of pandemic A(H1N1) 2009 influenza virus. Journal of Virology. 2010; 84:12069–12074. [PubMed: 20826688]
17. Mak GC, et al. Association of D222G substitution in haemagglutinin of 2009 pandemic influenza A (H1N1) with severe disease. Euro Surveillance. 2010; 15
18. Belser JA, et al. Effect of D222G mutation in the hemagglutinin protein on receptor binding, pathogenesis and transmissibility of the 2009 pandemic H1N1 influenza virus. PloS one. 2011; 6
19. Zhang Y, et al. Key molecular factors in hemagglutinin and PB2 contribute to efficient transmission of the 2009 H1N1 pandemic influenza virus. Journal of Virology. 2012; 86:9666–9674. [PubMed: 22740390]
20. Srinivasan A, et al. Quantitative biochemical rationale for differences in transmissibility of 1918 pandemic influenza A viruses. Proc Natl Acad Sci U S A. 2008; 105:2800–2805. [PubMed: 18287068]

21. Jia N, et al. Glycomic characterisation of respiratory tract tissues of ferrets: implications for its use in influenza virus infection studies. Journal of Biological Chemistry. 2014
22. Nicholls JM, Bourne AJ, Chen H, Guan Y, Peiris JS. Sialic acid receptor detection in the human respiratory tract: evidence for widespread distribution of potential binding sites for human and avian influenza viruses. Respiratory Research. 2007; 8:73. [PubMed: 17961210]
23. Chan RW, Chan MC, Nicholls JM, Malik Peiris JS. Use of ex vivo and in vitro cultures of the human respiratory tract to study the tropism and host responses of highly pathogenic avian influenza A (H5N1) and other influenza viruses. Virus Research. 2013; 178:133–145. [PubMed: 23684848]
24. Belser JA, et al. Pathogenesis and transmission of avian influenza A (H7N9) virus in ferrets and mice. Nature. 2013; 501:556–559. [PubMed: 23842497]
25. Richard M, et al. Limited airborne transmission of H7N9 influenza A virus between ferrets. Nature. 2013; 501:560–563. [PubMed: 23925116]
26. Pappas C, et al. Assessment of transmission, pathogenesis and adaptation of H2 subtype influenza viruses in ferrets. Virology. 2015; 477:61–71. [PubMed: 25659818]
27. Linster M, et al. Identification, characterization, and natural selection of mutations driving airborne transmission of A/H5N1 virus. Cell. 2014; 157:329–339. [PubMed: 24725402]
28. Chen Z, et al. Generation of live attenuated novel influenza virus A/California/7/09 (H1N1) vaccines with high yield in embryonated chicken eggs. Journal of Virology. 2010; 84:44–51. [PubMed: 19864389]
29. Soundararajan V, et al. Extrapolating from sequence--the 2009 H1N1 ‘swine’ influenza virus. Nature biotechnology. 2009; 27:510–513.
30. Yen HL, et al. Hemagglutinin-neuraminidase balance confers respiratory-droplet transmissibility of the pandemic H1N1 influenza virus in ferrets. Proc Natl Acad Sci U S A. 2011; 108:14264–14269. [PubMed: 21825167]
31. Reed LJ, Muench H. A simple method of estimating fifty percent endpoints. Am J Hyg. 1938; 27:493–497.
32. Zhou B, et al. Single-reaction genomic amplification accelerates sequencing and vaccine production for classical and Swine origin human influenza a viruses. Journal of Virology. 2009; 83:10309–10313. [PubMed: 19605485]
33. Nakamura K, et al. Sequence-specific error profile of Illumina sequencers. Nucleic Acids Res. 2011; 39:e90. [PubMed: 21576222]
34. Wang S, Sundaram JP, Stockwell TB. VIGOR extended to annotate genomes for additional 12 different viruses. Nucleic Acids Res. 2012; 40:W186–192. [PubMed: 22669909]
35. Li K, Stockwell TB. VariantClassifier: A hierarchical variant classifier for annotated genomes. BMC Res Notes. 2010; 3:191. [PubMed: 20626889]
36. Matsuoka Y, et al. African green monkeys recapitulate the clinical experience with replication of live attenuated pandemic influenza virus vaccine candidates. Journal of Virology. 2014; 88:8139–8152. [PubMed: 24807726]
37. Jayaraman A, et al. Decoding the distribution of glycan receptors for human-adapted influenza A viruses in ferret respiratory tract. PloS One. 2012; 7:e27517. [PubMed: 22359533]

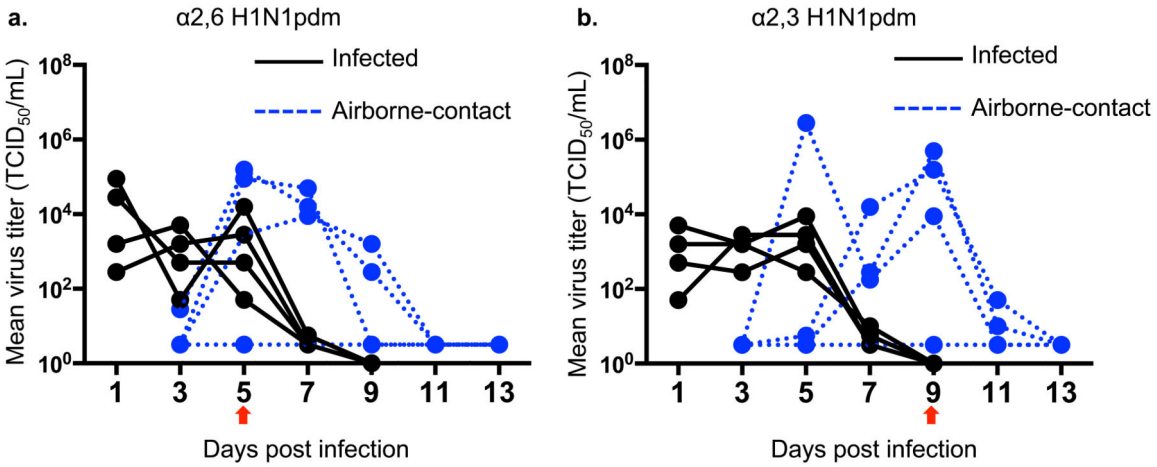

Fig. 1. Airborne transmission of receptor specific H1N1pdm viruses

Transmission studies were performed in double secure cages with perforated dividers[12]. One ferret in each pair was infected with 10^6 $TCID_{50}$ of the indicated virus, a naïve ferret (referred to as airborne-contact or AC) was introduced into the adjacent compartment 24 hours later. Nasal secretions were collected every other day for 14 days. Viral titers from the nasal secretions are graphed for each infected or AC animal. Transmission of α2,6 H1N1pdm (**a**) and α2,3 H1N1pdm (**b**) viruses was similar. The red arrow indicates the peak day of viral shedding for AC animals.

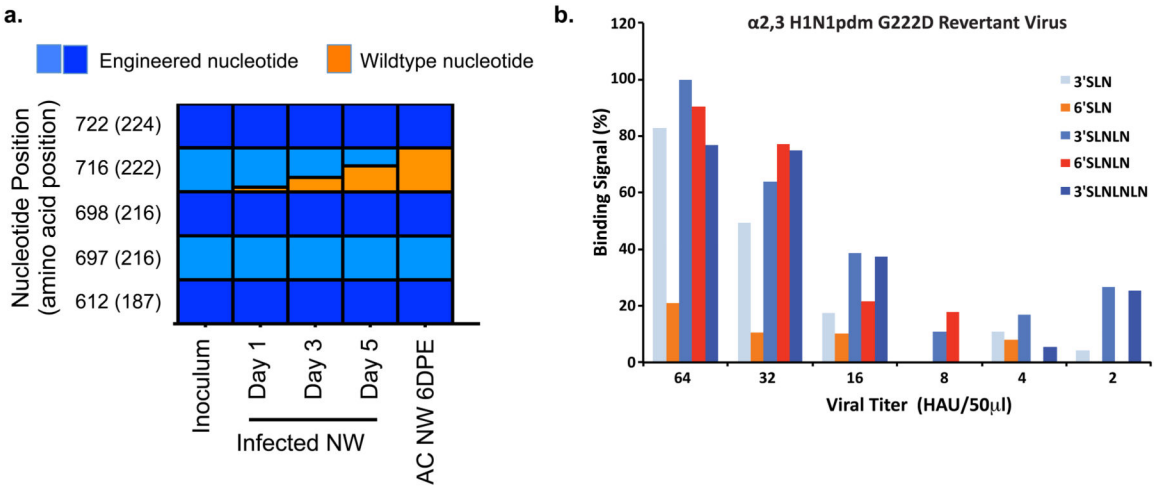

Fig. 2. Characterization of transmissible α2,3 H1N1pdm viruses

Deep sequencing of the α2,3 H1N1pdm inoculum, nasal wash (NW) from an infected ferret on 1, 3, and 5 DPI, and NW from one AC animal on 6 days post-exposure (DPE), representative of the 3 AC animals, revealed a reversion at residue 222 from G to D (**a**). Graphical representation of the proportion of reads at each engineered nucleotide is shown. Blue shading represents the α2,3 engineered nucleotide and orange represent the WT nucleotide residue. All other engineered nucleotides were maintained. A G222D reversion, in the context of the other engineered mutations, affects the glycan specificity of the α2,3 H1N1pdm virus (**b**). The glycans are indicated in the figure legend, orange colors represent α2,6SA and blue colors represent α2,3SA. H1 numbering is used for all amino acid positions.

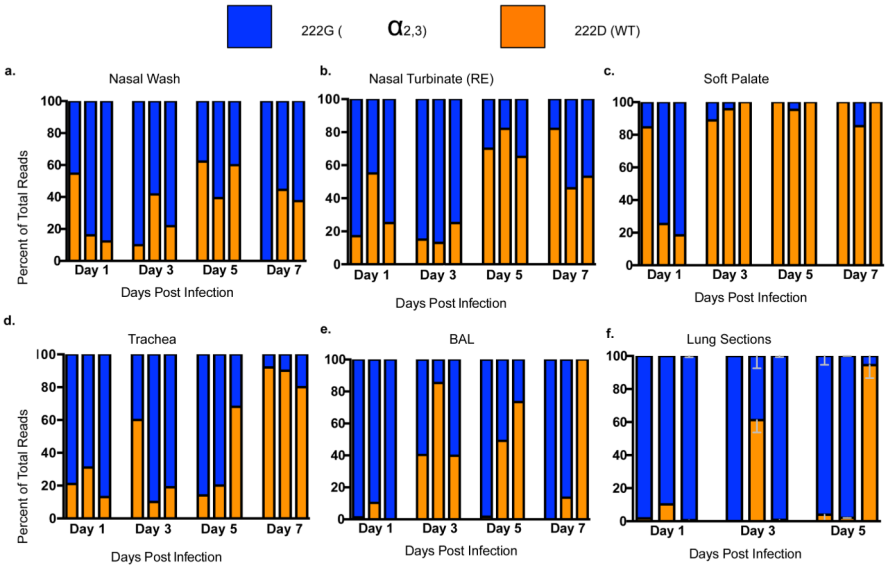

Fig. 3. Emergence of the α2,3 G222D H1N1pdm virus in the ferret respiratory tract

Different samples from the ferret respiratory tract: NW (**a**), respiratory epithelium (RE) of nasal turbinates (NT) (**b**), soft palate (**c**), trachea (**d**), bronchoalveolar lavage (BAL) (**e**), and combined right middle and left cranial lung sections (**f**) were collected on 1, 3, 5 and 7 DPI. The RE region of the NT is depicted in Extended Data Fig. 6h. The HA gene from virus populations in these samples were deep sequenced and the proportion of reads with D at position 222 is shown in orange, and G is shown in blue. Each bar represents a single animal. The standard error between the right and left lung sections is shown in **f**.

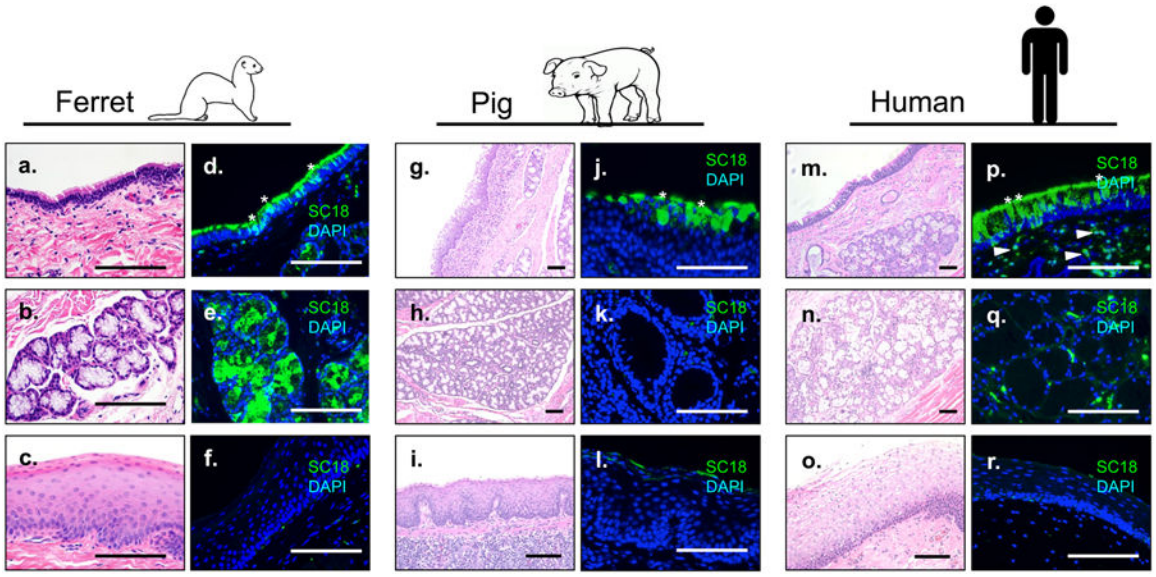

Fig. 4. Comparison of long-chain α2,6 SA expression in the soft palate of ferrets, pigs and humans

H&E staining of the soft palate from an uninfected ferret (**a-c**), pig (**g-i**) and human (**m-o**) highlights the nasopharyngeal, submucosal glands (SMG), and oral surfaces. Purified SC18 HA was used to define long-chain α2,6 SA in these sections from an uninfected ferret (**d-f**), pig (**j-l**) and human (**p-r**). Staining of the nasopharyngeal surface is depicted for each species across the first row, SMG in the second row and oral surface on the last row. A sialidase A treated control was run for each sample to ensure specificity of SC18 HA (not shown). Scale bars are 100μm in all images. Asterisks (*) highlight SC18 positive goblet cells and white arrowheads indicate SC18 positive plasma cells in human soft palate.